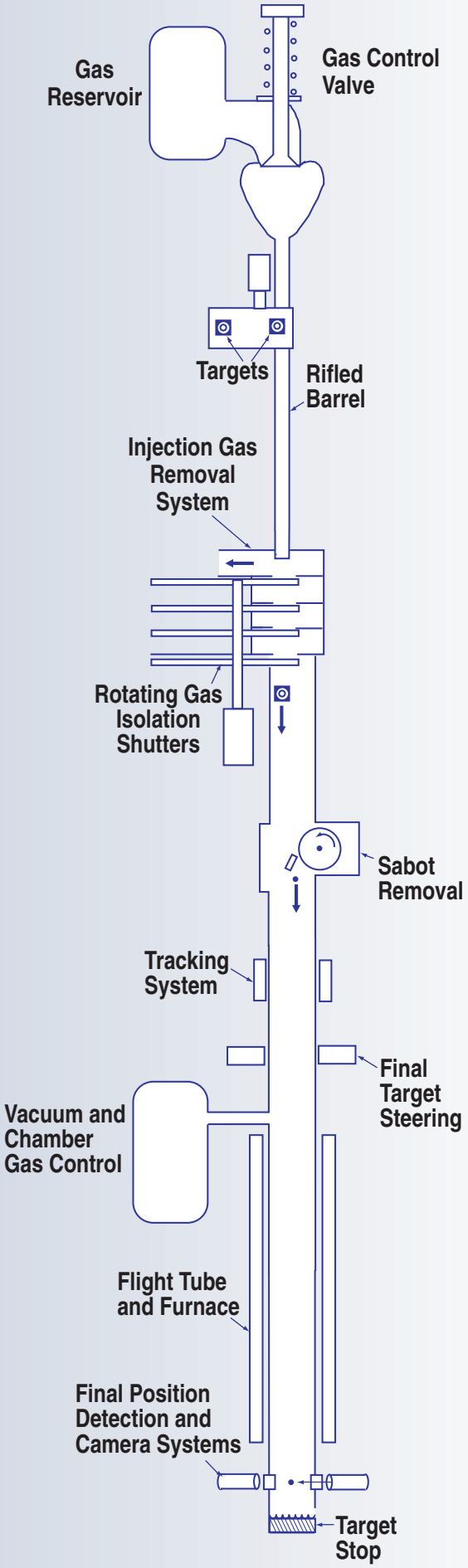

Target Injection System

FUSION RESEARCH AT GENERAL ATOMICS

ANNUAL REPORT

OCTOBER 1, 1999
THROUGH
SEPTEMBER 30, 2000

ADVANCED FUSION TECHNOLOGY RESEARCH AND DEVELOPMENT

GENERAL ATOMICS

DISCLAIMER

This report has been reproduced
directly from the best available copy

Available to DOE and DOE contractors from the
Office of Scientific and Technical Information
P.O. Box 62
Oak Ridge, TN 37831
Prices available from (615) 576-8401,
FTS 626-8401

Available to the public from the
National Technical Information Service
U.S. Department of Commerce
5285 Port Royal Road
Springfield, VA 22161

Cover Photo: Simplified schematic of experimental target injection and tracking system.

GA–A23599

ADVANCED FUSION TECHNOLOGY RESEARCH AND DEVELOPMENT

ANNUAL REPORT TO THE U.S. DEPARTMENT OF ENERGY

OCTOBER 1, 1999 THROUGH SEPTEMBER 30, 2000

by
PROJECT STAFF

Work supported by
U.S. Department of Energy
under Contract No. DE-AC03-98ER54411

GENERAL ATOMICS PROJECT 30007
DATE PUBLISHED: JUNE, 2001

CONTENTS

1. ADVANCED FUSION TECHNOLOGY RESEARCH AND DEVELOPMENT OVERVIEW 1-1

2. FUSION POWER PLANT DESIGN STUDIES 2-1

MHD Equilibrium and Stability 2-1
Transport Analysis using GLF23 and Toroidal Rotation Transport Study using NBI 2-3
Divertor and Wall Heat Loads 2-4

3. NEXT STEP FUSION DESIGN 3-1

Summary of FY00 Activities and Accomplishments 3-1
Disruption Specifications 3-2
Other Operations Issues 3-4

4. ADVANCED LIQUID PLASMA-FACING SURFACES (ALPS) 4-1

Modeling 4-2
Atomic Data Coordination 4-2
Core Transport and System Study 4-3
Optimum Aspect Ratio Designs 4-3
Planning for Next Year on the Tokamak Experiments Task 4-3
Summer Student and Consultant 4-4

5. ADVANCED POWER EXTRACTION STUDY (APEX) 5-1

Evolve Conceptual First Wall Blanket Design 5-1
APEX Interim Report 5-1
Evolve First Wall Blanket Design 5-1
Boiling Blanket Design 5-1
Transpiration First Wall Blanket Design 5-1
Germany Collaboration 5-2
Other Support 5-2
Review 5-3

CONTENTS (Continued)

6. PLASMA INTERACTIVE MATERIALS (DiMES) 6-1

Carbon Source in DIII–D 6-1
DIII–D Tiles 6-2
Li-Exposure Experiments 6-3
Solid Target Dedicated Experiment 6-5
First Wall Recycling 6-5
Planning for Next Year 6-5
DiMES System Maintenance 6-6
Summer Student 6-6

7. RADIATION TESTING OF MAGNETIC COIL 7-1

8. VANADIUM COMPONENT DEMO 8-1

9. RF TECHNOLOGY 9-1

Combline Antenna 9-1
Advanced ECH Launcher Development 9-2
International Collaboration 9-3

10. IFE TARGET SUPPLY SYSTEM 10-1

Background 10-1
FY00 Scope and Objectives 10-1
Target Injection and Tracking System Conceptual Design 10-1
Sabot Separation Experiment 10-3
Calculations of Target Heating and Drag 10-3
Summary of Accomplishments 10-5

11. ARIES INTEGRATED SYSTEM STUDIES 11-1

Background 11-1
Accomplishments and Activities 11-1

12. SPIN-OFF BROCHURE 12-1

LIST OF FIGURES

2-1. Cross-section of ARIES-AT power core configuration showing the proposed RWM control coil 2-2

6-1. Li sample exposure on DIII–D 6-4

7-1. Proposed test "coil" and model predictions 7-1

8-1. Vanadium brackets are part of the DIII–D strut protection tile assemblies 8-1

8-2. Vanadium alloy specimens behind DIII–D private flux divertor baffle 8-2

9-1. GA combline antenna mockup and water load 9-2

9-2. Remotely steerable launcher apparatus in low power testing at JAERI 9-4

10-1. Simplified schematic of experimental target injection and tracking system 10-2

10-2. The sabot isolates the capsule from warm propellant gas during acceleration and separates due to spring force after leaving the barrel 10-3

10-3. Photograph taken 5 ms after sabot release 10-4

10-4. Average target increase of outer ablator temperature for a target moving through a xenon-filled reaction chamber 10-4

10-5. Change in target position versus pressure for various fractional pressure variations 10-5

12-1. The spin-off brochure begins with explanations of fusion aimed at the interested but non-technical person 12-1

LIST OF TABLES

3-1. FIRE disruption and disruption-related design basis recommendations 3-3

Section 1

ADVANCED FUSION TECHNOLOGY RESEARCH AND DEVELOPMENT OVERVIEW

1. ADVANCED FUSION TECHNOLOGY RESEARCH AND DEVELOPMENT OVERVIEW

The General Atomics (GA) Advanced Fusion Technology program seeks to advance the knowledge base needed for next-generation fusion experiments, and ultimately for an economical and environmentally attractive fusion energy source. To achieve this objective, we carry out fusion systems design studies to evaluate the technologies needed for next-step experiments and power plants, and we conduct research to develop basic and applied knowledge about these technologies. GA's Advanced Fusion Technology program derives from, and draws on, the physics and engineering expertise built up by many years of experience in designing, building, and operating plasma physics experiments. Our technology development activities take full advantage of the GA DIII–D program, the DIII–D facility, the Inertial Confinement Fusion (ICF) program and the ICF Target Fabrication facility.

The following sections summarize GA's FY00 work in the areas of Fusion Power Plant Studies (Section 2), Next Step Options (Section 3), Advanced Liquid Plasma Facing Surfaces (Section 4), Advanced Power Extraction Study (Section 5), Plasma Interactive Materials (Section 6), Radiation Testing of Magnetic Coil (Section 7), Vanadium Component Demonstration (Section 8), RF Technology (Section 9), Inertial Fusion Energy Target Supply System (Section 10), ARIES Integrated System Studies (Section 11) and Spin-offs Brochure (Section 12). Our work in these areas continues to address many of the issues that must be resolved for the successful construction and operation of next-generation experiments and, ultimately, the development of safe, reliable, economic fusion power plants.

The work was supported by the Office of Fusion Energy Sciences, Facilities and Enabling Technologies Division, of the U.S. Department of Energy.

Section 2

FUSION POWER PLANT DESIGN STUDIES

2. FUSION POWER PLANT DESIGN STUDIES

This year the ARIES-AT reactor physics study focuses on issues related to ARIES-AT equilibrium, stability, transport, and divertor heat load. These are summarized below.

MHD EQUILIBRIUM AND STABILITY

In the equilibrium area, to allow an accurate evaluation of the divertor heat load, equilibria with a X–point at the plasma boundary have been computed using the EFIT code based on the reference limiter equilibrium. To evaluate the effects of the H–mode pressure and current profiles on MHD stability, equilibria with H–mode like profiles and X–point have also been generated by perturbing the L–mode like reference limiter equilibrium. Ideal stability analyses indicate that stability against the low $n = 1, 2$ modes are relatively insensitive to the presence of the X–point and the broader H–mode like pressure and current profiles. The location of the conducting wall required for stabilization against these modes remains similar. Stability against the high n ideal ballooning modes, which are limiting the L–mode like reference limiter equilibrium, is improved by the H–mode like profiles. With sufficiently high edge pressure gradient and bootstrap current, the equilibria have second ballooning stability access across most of the plasma volume.

The stability against the $n = 1$ resistive wall modes (RWM) is evaluated using the MARS code. The results indicate that a rotational drive $V/V_A > 0.08$ is necessary to keep the stability window open. Preliminary estimates indicate that 50–100 MW of ICH power may be needed to provide this rotational drive based on a mechanism proposed by Perkins [1]. An alternative intelligent shell feedback scheme to stabilize the $n = 1$ resistive wall modes (RWM) has also been evaluated. In this intelligent shell feedback approach, external coil currents are utilized to make the resistive wall appear almost ideally conducting to the plasma. Initial results indicate that the resistive wall can be made to be 90% effective to the $n = 1$ RWM by covering the resistive wall with 7 segments of poloical coils of equal poloidal coverage. The results suggest that the reference baseline case (which is at 90% of the ideal wall limit) is stable to the $n = 1$ RWM's with an intelligent shell.

A brief study of the RWM external feedback coil design based on the configuration used in DIII–D [2] has also been completed. The results indicates that it is essential to have the coil skin time $\tau_{L/R} > 10$ ms in order to keep the power requirement at a modest

level. This is shown in Fig. 1. The present design only considers modes with $n = 1$. RWM's with $n \geq 2$ have not been observed in DIII–D.

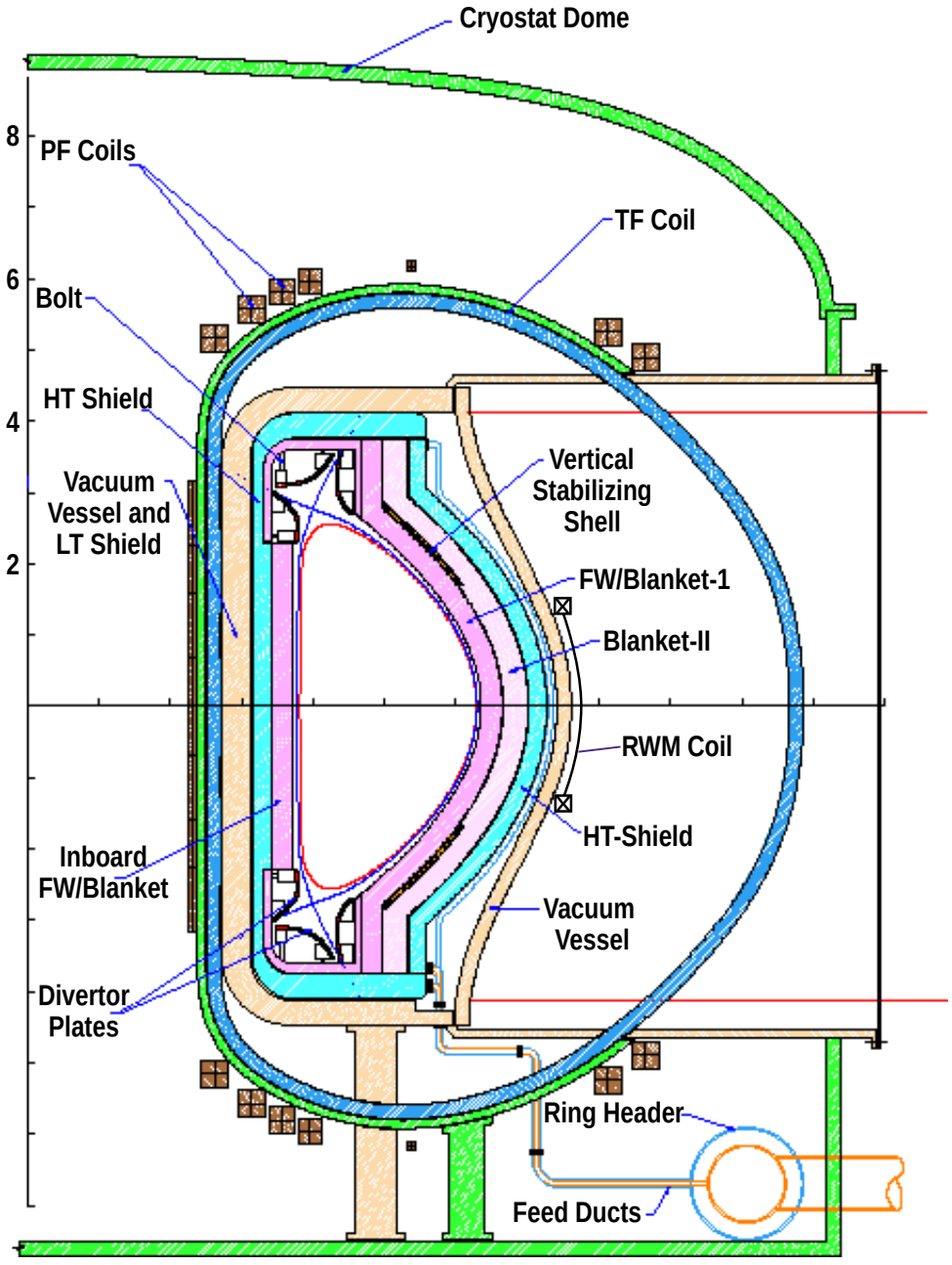

Fig. 2-1. Cross-section of ARIES-AT power core configuration showing the proposed RWM control coil.

The stability against the 5/2 neo-classical tearing modes and their control requirements are evaluated for the L–mode edge reference equilibrium using the modified

Rutherford equation which includes the effect of replacing the "missing" bootstrap current and the polarization threshold term. The results indicate that using radially localized electron cyclotron current drive (ECCD) to replace the missing bootstrap current at fixed Δ' is not effective due to the very high ARIES-AT bootstrap current fraction. Allowing the equilibrium current density to be modified by the radially localized ECCD so as to make Δ' more negative is more effective.

The stability against the intermediate *n* edge localized MHD modes has also been evaluated using the ELITE MHD stability code [3]. ELITE solves the edge ballooning equations which incorporate the effects of finite edge current and a proper treatment of the plasma-vacuum boundary. As expected, the L–mode edge reference equilibrium is found to be stable to the edge modes over a wide range of $n = 10–25$. On the other hand, the H–mode edge case is much closer to the edge instability boundaries. Although the equilibrium is stable to the pure ballooning modes, the additional "peeling" free energy, provided by the finite edge current, drives this equilibrium close to the marginal point for intermediate *n* stability. The H–mode edge results are consistent with the ELMing H–mode scenario as envisioned for ARIES-AT.

TRANSPORT ANALYSIS USING GLF23 AND TOROIDAL ROTATION TRANSPORT STUDY USING NBI

Predicting the transport in a new tokamak by projecting from a database of existing tokamaks is the method that has been used for all previous reactor design studies. In recent years an alternative method has become available with the advent of drift-wave based transport models. For the ARIES-AT design the GLF23 drift-wave based model [4] has been used to project the transport. This model has been shown to be about as accurate as the empirical scaling in predicting the global energy confinement time for a database of tokamak discharges. Both L–mode and H–mode discharges were included in the database.

Physics-based transport simulations using the GLF23 code indicate that the optimized pressure and current profiles can be sustained with an ELMing-H–mode like modestly peaked density profile. GFL23 transport model predicts global energy confinement which exceeds the ARIES-AT design requirement if the density profile is peaked. The energy confinement improvement is primarily due to Shafranov shift stabilization of drift-waves. The Shafranov shift causes an increase in the temperature gradient threshold for the drift waves but does not reduce the transport all the way to neoclassical. This has the advantage of giving improved transport without a localized steep gradient from which MHD instabilities can feed.

The torque density due to 50 MW of 120 keV neutral beams injected in the direction of the plasma current has been computed by the ONETWO transport code. A toroidal rotation ~ 500 km/s at the q=3 surface is needed to prevent the resistive wall mode for the baseline design point. The q=3 surface is very near to the edge at $\rho = 0.98$. This makes it impractical to achieve such a large rotation speed since the separatrix toroidal rotation is small and the rotation shear is limited by the large edge transport. The toroidal rotation due to the 50 MW of co-NBI was computed for this case but it made almost no difference at the q=3 surface. Toroidal momentum injection by NBI is not a practical means to suppress RWM's in ARIES-AT.

DIVERTOR AND WALL HEAT LOADS

In the divertor heat load area, power loading of the vacuum vessel is computed using the RADLOAD code. High radiated fraction, > 50%, of the total exhausted power is necessary to keep the peaked heat fluxes at a manageable level, < 10 MW/m^2. Impurity transport simulated using the MIST code assuming constant particle diffusivity indicates that a radiating mantle with 60%–70% radiation of the total exhausted power can be produced with a modest level of Argon or Krypton injected into the plasma.

A radiative divertor design has also been evaluated. Argon is chosen as the seeding impurity. Similar to neon, argon is expected to radiate reasonably well under ARIES-AT divertor and scrape-off layer conditions. However, in the edge region, argon radiates much more efficiently than neon. To reduce the peak divertor heat flux to the 5–6 MW/m^2 range, about 40% of the heating power is required to radiate in the divertor region. In this estimate, a fixed fraction of argon, $n_e^{Ar}/n_e = 0.26\%$, is assumed to be present in the SOL/divertor region.

REFERENCES

[1] F.W. Perkins, et al., "Generation of Plasma Rotation in a Tokamak by Ion-Cyclotron Absorption of Fast Alfvén Waves," Proc. IAEA Fusion Conference, Sorrento, Italy, October 2000.

[2] A.M. Garofalo, A.D. Turnbull, E.J. Strait, M.E. Austin, J. Bialek, *et al.*, Phys. Plasmas **6**, 1893 (1999).

[3] H.R. Wilson, R.L. Miller, *et al.*, Phys. Plasmas **6** (1999) 1925.

[4] R.E. Waltz, G.M. Staebler, W. Dorland, G.W. Hammett, M. Kotschenreuther, and J.A. Konings, Phys. Plasmas **4** (1997) 2482.

Section 3

NEXT STEP FUSION DESIGN

3. NEXT STEP FUSION DESIGN

This task provides physics analysis and other scientific and technical input to Next Step Options (NSOs) Studies for the US Fusion Science Program. Emphasis in this work is on options (design candidates) to obtain plasma behavior at high energy gain and for long duration operation pulses. The task scope established for FY00 is to provide definition of physics and plasma operation objectives, physics and plasma science assessments and definition of physics and other design requirements for U.S. NSO studies, especially as embodied in the FIRE (Fusion Ignition Research Experiment), is a national design study effort.

Activities in FY00 were funded at a level of approximately 0.2 FTE and were conducted on an approximately constant level-of-effort. Activities consisted primarily of continuing participation in the FIRE (Fusion Ignition Research Experiment) national design study effort and attendance at the FIRE Physics Issues Workshop held at Princeton Plasma Physics Laboratory in May 2000. A summary of disruption physics design basis specifications and disruption-related physics operation issues was presented and discussed at the workshop. Questions about the potential impact of the limited FIRE pulse repetition rate and number of pulses on physics operation issues were raised in a separate presentation.

SUMMARY OF FY00 ACTIVITIES AND ACCOMPLISHMENTS

Task activities in FY00 encompassed completing the defintion of the FIRE physics basis and performance projections. Attention in the first half of the year focused on plasma performance issues: achievable plasma energy gain ($Q = P_{fus}/P_{aux}$), sensitivity of performance to assumptions about density profile peaking and operational questions such as H–mode access with planned auxilary heating power. Tradeoffs between enhanced energy confinement (advanced tokamak operation) obtained at reduced plasma current and toroidal field and the corresponding extension of magnet and plasma current pulse length were examined in a parametric fashion. Summaries of the findings obtained on these performance and “mission envelope” issues were communicated to FIRE project management.

In the second half of FY00, activities focused on presentation and justification of physics-related specifications for disruptions, vertical displacement events (VDEs) and after-disruption conversion of plasma current to runaway electron current. A summary of

these recommendations was presented at the FIRE Physics Workshop (May 1–3, 2000 at Princeton Plasma Physics Laboratory) and a copy of the presentation plus associated "action items" and a draft FIRE "Disruption DDD (Design Description Document)" were made available on the FIRE website.

DISRUPTION SPECIFICATIONS

For FIRE vacuum vessel and in-vessel component design purposes, the most important disruption-related parameters are 1) the durations of the thermal and magnetic energy quenches and the partitioning of the corresponding plasma energies among the divertor and first wall (FW) surfaces and 2) the magnitude and toroidal asymmetry of the poloidal ("halo") current flow in conducting in-vessel structures that arises owing to rapid plasma vertical instability. The possibility of localized runaway deposition is another important consideration for the design of at-risk plasma facing component (pfc) surfaces.

Table 5-1 summarizes the recommended physics design bases for these and related parameters in FIRE. The basis for this table is a high-Q DT plasma, with initial current I_{p0} = 6.5 MA, as obtained at B = 10 T with q_{95} = 3.0. This plasma produces 200 MW fusion power at $\beta_N = \langle\beta\rangle aB/I \approx 2.5$: thermal and magnetic energies W_{th} and W_{mag} are respectively about 33 MJ and 35 MJ. Here W_{mag} includes the ex-plasma magnetic energy within the FIRE vacuum vessel. This vacuum vessel and the associated passive stabilizing structures, which have an effective toroidal L/R time constant of ~60 ms, determine the passive stability of the plasma with respect to n = 0 modes (and hence the time-scale of VDE evolution) and also limit the in-vessel magnetic energy dissipation from the disruption or VDE current quench to ~W_{mag}.

The parameters given in Table 1 are generally the maximum or "worst-case" limits expected. But as the table makes clear, there are appreciable uncertainties in all of the FIRE disruption and disruption-related predictions, so it will be prudent for vessel and in-vessel component designers to examine the consequences of the range of possible parameters.

TABLE 3-1
FIRE Disruption and Disruption-Related Design Basis Recommendations

Parameter	Value (Range)	Comment
Frequency	10% (10-30%) per pulse	30% for plasma development ≤ 10% for mature (repetitive) operation
Number (3,000 full perform. attempts)	300 (900)	300 at full W_{th} and W_{mag}, balance at ≤ 0.5 W_{th} and full W_{mag}
Thermal energy	33 MJ	For typical 200 MW plasma
Thermal quench duration	0.2 (0.1–0.5) ms	Single or multi-step thermal quench, see text
Fraction of W_{th} to divertor	80–100%	By conduction to targets, up to 2:1 toroidal asymmetry, see text
Fraction of W_{th} to FW (baffle)	≤ 30%	By radiation (to FW) or conduction (to baffle)
In-divertor partition (inside/outside)	2:1 – 1:2	For SN plasmas. Significant uncertainty: see text. No data for DN plasmas
Poloidal localization in divertor	3-x normal SOL; (1-x to 10-x)	Incident energy, with up to 2:1 toroidal asymmetry. Plasma shielding and re-radiation will likely redistribute in-divertor energy
Magnetic energy	35 (?) MJ	For 6.5 MA, total out to VV
Current quench duration	6 (2-600) ms	Duration ≥30 ms: more-severe VDE and halo current
Maximum current decay rate	3 MA/ms	May occur only during fastest part of current quench; typical maximum rate ~1 MA/ms
Fraction of W_{mag} to FW, by radiation	80–100%	By radiation, with poloidal peaking factor ~2
Fraction of W_{mag} to FW, by localized conduction	0-20%	From VDE: depends on VDE evolution and in-vessel halo current. Hot-plasma VDEs may also deposit ~0.2-1.0W_{th} on localized portion(s) of FW. Toroidal alignment critical
VDE frequency	TBD (??? 1% of pulses, or 10% of disruptions???)	Presently very uncertain. May be able to maintain vertical position control after thermal quench. But margin/noise sensitivity is uncertain. Control failure will result in VDE or loss of after-thermal-quench control
Halo current fraction $I_{h,max}/I_{p0}$	0.4 (0.01-0.50)	Highest value may apply (depends on passive stabilizer configuration)
Toroidal peaking factor	2 (1.2 ≤ TPF ≤ 4)	TPF up to 2 yields '$\sin\phi$' distribution; TPF > 2 yields 'localized filament'
$(I_{h,max}/I_{p0})$*TPF	≤ 0.50 (typical maximum)	Data bound is ≤ 0.75 (see text)
Runaway electron current (following disruption or fast shutdown)	50% I_p (0-50%)	Highly uncertain. I_{RA} > 1 MA requires ≥ 1 A seed source. Not expected in thermal plasma, but pellet shutdown may seed avalanche. MHD fluctuations may offset part or all of avalanche growth.
Runaway energy	~15 MeV	Limited by knock-on avalanche
Localization of runaway deposition	≤ 1 m^2	Poloidal localization to a ~0.1 m (poloidal) section of the FW or divertor target expected; toroidal localization depends on pfc and wall alignment to toroidal field

The presentation and follow-up discussion identified two key FIRE-relevant lacks in the present physics basis understanding of disruptions: 1) The generally poor quality of thermal quench duration and energy accountability and 2) the specific lack of thermal

quench accountability data for double-null (rather than single-null) plasma configurations. Renewed study of these aspects of disruption in present double-null capable experiments in the U.S. (Alcator C-Mod and DIII–D) could reduce the present large uncertainty in the FIRE divertor target thermal quench loading.

OTHER OPERATION ISSUES

A separate presentation made at the worksop raised questions about the plasma operation and experiment impact of the FIRE pulse repetition rate, which will be approximately 0.33 pulses per hour (i.e., 1 pulse every three hours) owing to the need to recool the toroidal field (TF) coil to liquid nitrogen temperature after a full-field (10 T) pulse. The projected FIRE pulse rate will be about 1/10th of the repetition rate of present "medium" and "large"-size tokamak experiments. In addition, the annual number of full-power DT burn pulses will be limited to about 300 pulses per year if the 6 TJ FIRE lifetime fusion energy yield limit (set by TF insulation irradiation) is to be evenly apportioned over a 10 year DT operation period. Again, 300 pulses per year is about 1/10th of the corresponding annual pulse quota of present tokamak experiments. The FIRE pulse rate and annual number limitations may limit the type and depth of "burning plasma" physics studies that can be carried out in FIRE, especially if study of "advanced tokamak" operation modes is included in the objectives of the FIRE program.

Activities in the 4th quarter of FY00 were 1) continued participation in the FIRE national design study effort, and 2) submission of input and comments on FIRE physics issues and bases for papers submitted on behalf of the FIRE national team to the IAEA (International Atomic Energy Agency) biannual fusion conference and the SOFT (Symposium on Fusion Technology) fusion technology conference.

Section 4

ADVANCED LIQUID PLASMA-FACING SURFACES (ALPS)

4. ADVANCED LIQUID PLASMA-FACING SURFACES (ALPS)

During this fiscal year we worked in the areas of edge modeling, atomic data coordination, impact of low recycling edge on core performance, and modeling of power and test reactor performance. A 3-D neutral scattering model was implemented in MCIP and compared to the PISCES CD_4 injection experiments. Both the Ehrhardt/Langer and the Alman/Ruzic models predict CD penetration depths that compare favorably with the PISCES experimental data when Bohm diffusion is used to specify the radial diffusion coefficient of the hydrocarbon molecules.

We modified the MCI point source launch model to better represent the Li DiMES sample experiment. Furthermore, both ADAS and ADPAK lithium data files were loaded into the MCI code. For the evaluation of Sn as the plasma facing material, the ADPAK program was modified to extract total radiated power rates from the ADPAK database. The Sn data was compared to radiated power curves supplied by D. Post and was sent to J. Brooks at ANL for the modeling of the Sn DiMES exposure experiment that is proposed for DIII–D. A data table was also prepared and distributed to the ALPS Modeling Group. This data table contains the total electron impact ionization rates for SnI→SnII, SnII→SnIII, and SnIII→SnIV over a range of electron temperatures from 1.08 to 933.3 eV.

We used the ONETWO core modeling to study the high and low recycling edge conditions of the ITER reference design. Results have highlighted the importance of understanding how the pedestal physics affects the core profiles. Preliminary results also show that the high recycling case is very similar to the ITER design. The low recycling case produces nearly twice the net electrical power and a corresponding reduction in the cost of electricity by about 30%. These are very preliminary results and, in addition to the physics issues, we need to understand further the differences in the input assumptions used for the ONETWO and system code calculations.

Using our system code, we completed the mapping of superconducting and normal conduction coil tokamak power and test reactors as a function of aspect ratio and elongation. We found that the power reactors have a minimum cost of electricity at aspect ratio around 2 for both normal conducting and superconducting coil designs. This led us to recommend that the next step D-T machine could be a 200 MW fusion, A=2, κ=3 design at a cost of about ~$640M. These results were reported at the IAEA meeting in Sorrento, Italy.

MODELING

A 3-D neutral scattering model was implemented in MCIP and compared to the PISCES CD_4 injection experiments. Initially, very little difference was found compared to previous simulations, and the mismatch between the calculated and experimental results persisted. A good match of PISCES experimental results was found with both the Ehrhardt/Langer and the Alman/Ruzic models when Bohm diffusion is used to specify the radial diffusion coefficient of the hydrocarbon molecules. The simulations appear to be most sensitive to the mean-free path of the initial methane molecule. We looked at the detailed physics (reaction rates, neutral collisions, and force balance) of the methane molecule in order to determine which processes dominate the penetration statistics of CD molecule transport. We have also identified an analytic form for the radial diffusion coefficient in PISCES based on published experimental data and have implemented it in the code.

We modified the MCI point source launch model to better represent the Li DiMES sample experiment. Both ADAS and ADPAK lithium data files were loaded into the MCI code. For the evaluation of Sn as the plasma facing material, the ADPAK program was modified in order to extract total radiated power rates from the ADPAK database. Total radiated power rates were also extracted for Li and Sn. The Sn data was compared to radiated power curves supplied by D. Post and was sent to J. Brooks at ANL for making radiated power estimates for a Sn DiMES exposure experiment that is proposed for DIII–D.

ATOMIC DATA COORDINATION

A data table was prepared and distributed to the ALPS Modeling Group containing the total electron impact ionization rates for SnI→SnII, SnII→SnIII, and SnIII→SnIV over a range of electron temperature from 1.08 to 933.3 eV. A 1-D Monte Carlo code was developed for the calculation of Li thermalization times, ionization mean free path length, and spatial charge state distributions as a function of T_e. This data is needed to assess the impact of kinetic transport effects in simulations of liquid lithium target plates using the UEDGE code.

CORE TRANSPORT AND SYSTEM STUDY

A two point density scan was completed with the ONETWO code using SOL-core boundary conditions designed to represent the effects of liquid lithium divertor targets (i.e., low recycling UEDGE SOL solutions) in a reactor plasma. Solutions are very sensitive to the pedestal transport coefficients that allowed us to obtain stable edge profiles and steady-state conditions with both the high and low recycling chamber wall conditions. The low recycling case shows a substantial increase in T_e and T_i on axis compared to the high recycling case. The energy confinement time increases from 3.38 s to 5.09 s when going from the high to low recycling case. In addition, the DD neutron production rate increases from 2.06×10^{18} s^{-1} to 7.72×10^{18} s^{-1} and the bootstrap fraction increases from 28.8% to 65.5% in going from the high to low recycling case. The steady-state operating point found for the high recycling case has a Q_{DT} of 58.2 with an H(89p) of 2.22 compared to a Q_{DT} of 115.7 with an H(89p) of 3.67 in the low recycling case. While these preliminary results look promising for liquid lithium target divertor plates, it should be kept in mind that the core-pedestal transport physics, fueling, impurity content and pedestal-SOL coupling assumptions being used in these simulations require additional testing and that the MHD stability of these solutions needs to be evaluated.

OPTIMUM ASPECT RATIO DESIGNS

Using our system code, we completed the mapping of superconducting and normal conduction coil tokamak power and test reactors as a function of aspect ratio and elongation. We found that power reactors have a minimum cost of electricity at an aspect ratio around 2 for both normal conducting and superconducting coil designs. This led us to recommend that the next step D-T machine could be a 200 MW fusion, aspect ratio equals to 2, and elongation equals to 3 design at a cost of about $640M.

PLANNING FOR NEXT YEAR ON THE TOKAMAK EXPERIMENTS TASK

In response to the assigned task of Tokamak Experiments, C. Wong drafted a charter of this task, which focuses on the impact of lithium or other wall material on the other physics-related disciplines. The lithium or other wall material is treated as a perturbation to different areas of tokamak physics.

SUMMER STUDENT AND CONSULTANT

D. Alman of the University of Illinois joined us for the summer and, with guidance from T. Evans, completed the comparison between two molecular dissociation models with the PISCES data. Dr. Daniel Finkenthal from California State University-San Marcos initiated the kinetic modeling of the UEDGE code.

Section 5

ADVANCED POWER EXTRACTION STUDY (APEX)

5. ADVANCED POWER EXTRACTION STUDY (APEX)

We completed the preparation and review of the APEX interim report and we coordinated the EVOLVE, W-alloy lithium vapor cooled first wall and blanket design.

EVOLVE CONCEPTUAL FIRST WALL BLANKET DESIGN

APEX INTERIM REPORT

The APEX interim report review and preparation were completed.

EVOLVE FIRST WALL BLANKET DESIGN

We participated in the planning of the FY00 APEX program and were asked to lead the Task-IV refractory material design for FY00. Task IV focused on the vaporized Li first wall and blanket design. Design tasks were formulated and conference calls were used to coordinate different sub-tasks.

BOILING BLANKET DESIGN

John Murphy and Mike Corridini of UW analyzed the boiling lithium blanket option of the EVOLVE design. Based on the calculated superficial gas velocity, they determined that boiling lithium can be approximated by the churn-turbulent flow regime. Results show that the maximum boiling void fraction can be >65% at a pressure of 0.37 atm. With higher applied pressure of 1.7 atm., the void fraction can be reduced to ~60%. A vapor channeling model was suggested by S. Malang of FZK. Applying this model, the UW team showed that the lithium vapor volume fraction could be reduced from 65% to less than 12%. To confirm the results, they identified the need to investigate experimentally the regime of stable boiling in the presence of a magnetic field. The impact of higher void fraction would only increase the blanket radial thickness by about 10 cm outboard and 5 cm inboard.

TRANSPIRATION FIRST WALL BLANKET DESIGN

For the W-alloy first wall design, Leopold Barleon set up the analysis tools to evaluate the transpiration-cooled option. The lithium is superheated and converted to vapor at the low-pressure side of the capillary openings. Trade off studies on various performance parameters determined the dimensions of various first wall components.

Without boiling, we found that 1200°C lithium vapor could be generated by superheating the lithium while removing the deposited nuclear energy from surface heat flux and neutron wall loading by careful selection of the lithium layer thickness at the first wall while in the blanket. Most of the critical issues were identified and all the key thermal-hydraulics estimates were done. Barleon compared the toroidal and poloidal flow transpiration-cooled first wall designs. Due to the length of the flow path, the toroidal flow design has high maximum vapor outlet velocity of > 500 m/s at the first wall and the poloidal flow design has a much lower corresponding outlet velocity of 32 m/s. The poloidal design also has a coolant superheat of 46.5°C, which is lower than the 72.1°C required by the toroidal design. For the transpiration-cooled FW/blanket design options the key technical unknown is the quantification of the lithium superheat from the W-surface and in the bulk lithium slab.

In the area of crack evaluation, S. Majumdar of ANL showed that the EVOLVE W-alloy first wall design can withstand ~1000 cracks with initial crack width of 10 μm and a crack length of 25 mm before major impact would be felt by the plasma due to the effect of fuel dilution.

High afterheat from W-alloy continues to be a safety concern. The safety team at INEEL considered various means of passively removing the afterheat from the first wall and blanket, and a natural circulation lithium loop was identified as a possible option.

GERMANY COLLABORATION

Dr. Leopold Barleon, retired from FZK of Germany, worked with us for a total of three months. He also went to Sandia National Laboratory to work with R. Nygren on identifying possible experiments to determine the superheating of lithium. S. Malang of FZK , in addition to attending project meetings, traveled to INEEL, Idaho, University of Wisconsin in Madison, Wisconsin and GA in San Diego to consult on the EVOLVE design.

OTHER SUPPORT

GA’s system code was used to assess the radiation fraction of a low recycling edge power reactor. Kr was used as a core radiator to reduce the transport power to the divertor. Results were sent to the APEX Task III team for use in their evaluation.

REVIEW

Sam Berk of OFES reviewed our fusion technology program on July 27th.

CONFERENCES/MEETINGS

1. In February C. Wong attended the APEX/FHPD workshop in Japan and presented the status report of the EVOLVE design.

Section 6

PLASMA INTERACTIVE MATERIALS (DiMES)

6. PLASMA INTERACTIVE MATERIALS (DiMES)

After the DIII–D brainstorming planning exercise at the beginning of the fiscal year, our DiMES program was allotted two half-day dedicated run times for FY00. We then continued to plan and perform other piggyback experiments as reported below. We investigated the potential source of core carbon in DIII–D and eliminated possible contributions from divertor erosion from detached plasma shots and chemical erosion from the first wall. The core concentration remains constant. An experiment was carried out to study recycling and carbon sources at the main wall. Results showed that mid-plane recycling and total carbon influx increased strongly with decreasing gap width, but we are still uncertain about the mechanism that would explain the core carbon contribution from the chamber wall. Detailed analysis of the DiMES exposure of lithium sample experiments shows the increased out-flux of lithium from the solid to liquid state, the clear quantification of the J×B effect during ELMs on the liquid lithium and the measurement of lithium in the plasma core. Results were also obtained from Raman spectroscopy and X-ray Photoelectron Spectroscopy on characterizing the surface of DIII–D tiles. These results show signs of reduced chemical erosion and strong evidence for major modifications of the graphite surfaces caused by both boron and plasma deposition. In another series of dedicated experiments, we successfully exposed our solid surface DiMES sample to six very repeatable H–mode shots. A controlled amount of neon was injected to reduce the peak heat flux by a factor of 2.5 with a divertor floor temperature of about 4 eV. Improved plasma confinement was also observed. Preliminary results indicate the highest measured erosion rate of carbon compared to earlier results was obtained in this experiment.

CARBON SOURCE IN DIII–D

We investigated the potential source of core carbon in DIII–D and eliminated possible contributions from either divertor erosion from detached plasma shots or chemical erosion from the first wall. A summary of this investigation is included here. We reviewed all the erosion/redeposition results from similar ELMing H–mode DiMES exposures in the last seven years, and found net erosion from attached plasma shots on most of the outboard divertor. During the same period, the contribution due to chemical erosion was found to decrease by 20 fold because of boronization. Therefore the carbon source cannot be from chemical erosion. For detached plasma shots, essentially no erosion was measured at the outer and inner divertors, including the private flux region.

The core carbon concentration was measured to be nearly constant for all the attached and detached plasma shots. This can only mean that there is a source of carbon other than the lower divertor. The most likely explanation is the contribution from the chamber wall.

The mid-plane SPRED diagnostic was used to look at the intensity of carbon sources coming from the first wall. Results show: 1) the inferred flux of carbon at the mid-plane is consistent among the different charge state /lines measured (CII, CIII, CIV), 2) this influx of carbon has not changed over the last seven years, and 3) the apparent carbon erosion yield at the first wall (by comparing to recycling hydrogenic light at the mid-plane) is about 1%. The apparent magnitude of the flux, if integrated over the entire first wall, is quite large. This shows carbon contribution from the chamber wall. However, we have not yet identified the mechanism of core carbon contribution from the chamber wall. We will continue to focus our DiMES effort in FY01 to resolve this uncertainty.

DIII–D TILES

Extensive work was performed on characterizing the surface characteristics of DIII–D tiles. In summary, results show signs of reduced chemical erosion and strong evidence for major modifications of the graphite surfaces caused by both boron and plasma deposition. The work was carried out at PISCES and at the UCSD Center for Magnetic Recording Research.

Results from Raman spectroscopy and XPS (X-ray Photoelectron Spectroscopy) for the exposed DIII–D tiles are summarized in the following:

1. Row 2 tiles removed from the upper divertor (i.e. outer strikepoint position for pumping with upper single-null plasmas) were found to have large surface concentrations (> 50%) of clear crystals embedded in the graphite. These have been clearly identified as boric acid (H_3BO_3), and likely result from boron oxide (B_2O_3) reacting spontaneously with moisture after exposure to the atmosphere. This is a clear indication on the large concentration of boron on these tile surfaces, despite the fact that this region receives large D flux/fluences because of its position at the strike point. Also the chemical bonding/stability of crystal-like structures seem to be resistant to chemical erosion.

2. A large Raman fluorescence feature appears in all plasma-facing surfaces of the tiles but not on the backs of tiles. This is usually caused by semiconductor-like defects in the graphite structure and denotes a significant presence of oxides, carbides or other impurities in the graphite.

3. Raman spectroscopy of the lower divertor graphite surfaces gives results essentially identical to those found with laboratory produced chemical vapor deposited (CVD) diamond-like films rather than crystalline graphite. This is another indication of substantial chemical changes to the surfaces.

4. Raman spectroscopy of a tile section removed from the DIII–D outer mid-plane shows several features similar to boron carbide (B_4C) as well as diamond-like carbon film.

5. XPS of the lower divertor tiles shows a C line feature that is 3–4 times wider than spectra obtained from virgin graphite. The broadening appears to occur to both lower and higher energies and is likely the result of the blending of several line features that cannot be distinguished by the XPS technique. Typically, lower energy features are indicative of carbide formation, another indication of significant changes to the surface bonding of the carbon.

It was discovered that the boric acid crystals previously found on the removed upper divertor tiles were also present, but unnoticed in earlier measurements, on the row 4 tiles removed from the lower divertor in 1998. This qualitatively indicates substantial modification of surface chemistry in the lower divertor tiles which have contributed to reduced chemical erosion yield over the last eight years.

Li-EXPOSURE EXPERIMENTS

We exposed two Li samples. The first Li sample we received from SNL had an exposed edge of stainless steel. To reduce the amount of exposed metal we refilled the lithium on the DiMES sample, but during the process the sample was contaminated with air. The contaminated Li-sample was exposed to the plasma as a piggyback experiment. We could not get rid of the surface material (Li_2O, LiH and/or Li_3N) with helium glow discharge or by high power sweeping the plasma strike point, and were not able to melt the lithium material. A second Li-sample was prepared. This experiment was scheduled after the DIII–D vessel was boronized. During the helium glow discharge process to reduce the content of boron on the vessel surface, the DiMES sample was unexpectedly inserted, resulting in the removal of the Li from the sample, apparently due to J×B forces associated with ELMs. The edge of the Li stainless steel holder was severely eroded. Based on this experience we have taken measures to prevent this unexpected insertion from happening again by improved sample location indication and by not exposing the

stainless steel lithium holder. We will try to expose a few well-controlled low power plasma discharges on a new Li-sample without the stainless steel lip in FY01.

J.P. Allain from the University of Illinois, with guidance from D.G. Whyte, analyzed the data of the three lithium exposure experiments. Analysis was based on Langmuir probes, divertor Thomson scattering, infrared (IR) thermography data, the interpretation of lithium spectroscopy data and thermal analyses. They found that the lithium would be melted under a heat flux of ~1–2 MW/m^2 in about a second. At this heat flux and a poloidal current density > 10 kA/m^2, with a magnetic field strength of about 2 T, the J×B body force would remove the 0.1 to 0.2 mm thick layer of lithium. The lithium exposure conditions on DIII–D are shown in Fig. 6-1. Going from top to bottom of the five panels, the first panel shows the neutral beam injected power and the D_α emission during the discharge; the second panel shows the distance of the strike point from the DiMES

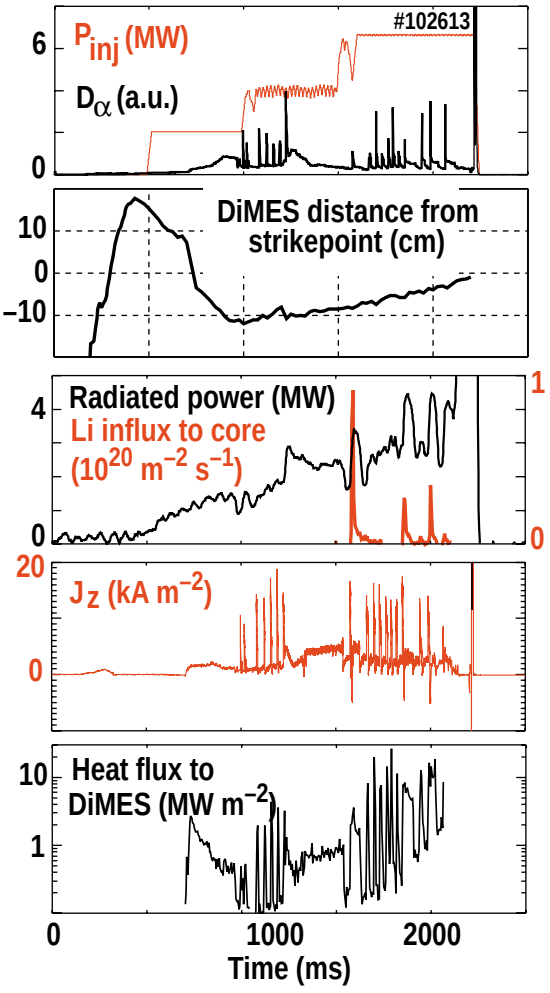

Fig. 6-1. Li sample exposure on DIII–D.

sample; the third panel shows the radiated power and the influx of lithium to the core especially during the reversed current density in the vertical direction as shown in the forth panel; and the fifth panel shows the heat flux to the DiMES sample during the discharge. Lithium was measured in the core plasma, even though the lithium sample area is about 10^{-4} of the lower divertor area on DIII–D. Results were sent to UCLA for liquid metal movement modeling.

SOLID TARGET DEDICATED EXPERIMENT

We exposed our solid surface DiMES sample to six very repeatable H–mode shots. A controlled amount of neon was injected to reduce the peak heat flux by a factor of 2.5 with a divertor floor temperature of about 4 eV. Improved plasma confinement was also observed. The exposed sample had V and W coatings. The sample has been sent to SNL-A for examination. Preliminary results indicate the highest measured erosion rate of carbon yet obtained was for the experiment with detached plasma at the divertor generated with the injection of neon. Detailed analyses are continuing.

FIRST WALL RECYCLING

An experiment was carried out to study recycling and carbon sources at the DIII–D main chamber wall. Diagnostics were focused near the outer mid-plane scrape-off-layer (SOL), while a scan of the outer gap from 2.5 to 10 cm was performed on a lower single-null plasma. Preliminary analysis showed that mid-plane recycling and total carbon influx increased strongly with decreasing gap width. Significant and uniform chemical CD emission was also found in the main plasma SOL. The core carbon concentration increased from ~0.75% to ~1.3% as the gap width decreased from 10 to 2.5 cm. These results indicate qualitatively that the main wall is an important location for plasma-wall interaction and impurity generation.

PLANNING FOR NEXT YEAR

We started to plan for next year's DiMES experiments. Fourteen experiments were proposed. Five are considered as dedicated experiments. They are the Li sample with controlled low power discharges, the Sandia National Laboratory divertor W-rod experiments, the detached plasma experiment with injection of higher-Z gas like Ar, the Sn coating experiment and the continuation of the leading edge experiment. We will prepare the presentation for these dedicated experiments for the DIII–D brainstorming

meeting on November 8–10, 2000. A summary presentation will also be prepared for the piggyback experiments.

DiMES SYSTEM MAINTENANCE

The DiMES system was re-calibrated and operating quite well in 2000. The lithium exposure Hazardous Work Authorization (HWA) was updated and accepted by the DIII–D safety committee for 2001.

SUMMER STUDENT

J.P. Allain from University of Illinois spent the summer at GA to analyze the results of the exposed lithium experiments.

CONFERENCES/MEETINGS

1. D.G. Whyte attended the APS-DPP meeting in Seattle, November 15–20, 2000.
2. C.P.C. Wong attended the NSTX forum held at PPPL on January 31 to February 2, and proposed for the DiMES team a material probe, similar to DiMES in DIII–D, to be installed at the lower divertor of NSTX.
3. D.G. Whyte participated at the Carbon workshop in Germany and presented results on chemical erosion.
4. C.P.C. Wong and D.G. Whyte made presentations at the DOE/OFES PFC peer review that was held at Sandia National Laboratory.
5. C.P.C. Wong attended the U.S./Japan workshop on high heat flux components and presented the recent results on DiMES.

PUBLICATIONS/REPORTS

1. W. Wampler, *et al.*, "Suppression of Erosion in the DIII–D Divertor with Detached Plasma," Proc. 14th International Conference on Plasma Surface Interactions in Controlled Fusion Devices, May 22–26, 2000 in Rosenheim, Germany. To be published in J. Nucl. Mater.
2. D.G. Whyte, *et al.*, "Reduction of Divertor Carbon Sources in DIII–D," Proc. 14th International Conference on Plasma Surface Interactions in Controlled Fusion Devices, May 22–26, 2000 in Rosenheim, Germany. To be published in J. Nucl. Mater.

Section 7

RADIATION TESTING OF MAGNETIC COIL

7. RADIATION TESTING OF MAGNETIC COILS

Study of radiation induced EMF (RIEMF) continued in FY00. Work included (1) a review of models and measurements of the effect of gamma and neutron fluxes creating spurious signals on test coils and (2) developing a model and test coil geometry which could be used in further tests to better confirm the physics of the source of the spurious voltages.

The proposed further test is based on a test coil with a slab geometry, shown below, and the assumption of the gamma or neutron flux acting as a beta emitter of energetic electrons in the MgO insulators. By symmetry, the Ni plates of the "coil" receive twice the flux of energetic electrons emitted as the stainless steel plates of the "shield" and tend to charge negatively with respect to the stainless steel plates which are grounded. A simplified geometry, such as this, can fit the materials constants and confirm any model predictions for more realistic coaxial cable coils, for example. Temperature effects can also be modeled as dependences of the coefficients on T.

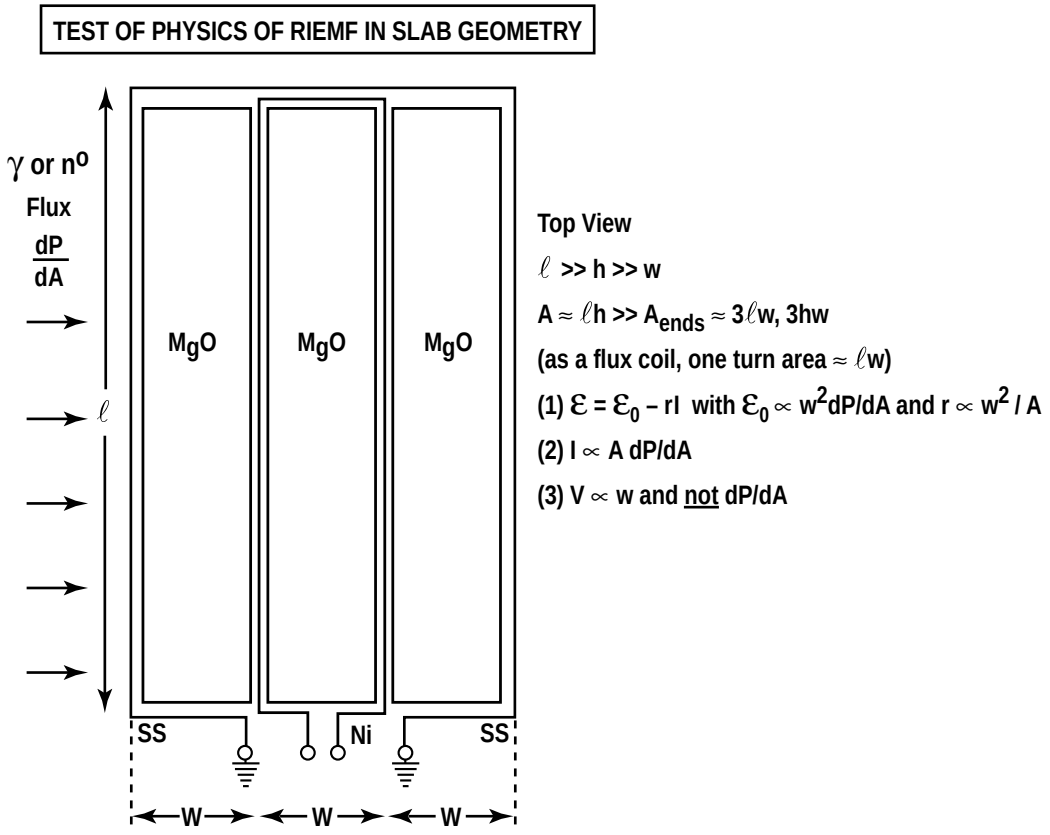

Fig. 7-1. Proposed test "coil" and model predictions.

CONFERENCES/MEETINGS

1. IAEA Three Large Tokamak Workshop for Burning Plasma Experiments, Naka, Japan, September 18–21, 2000.

Section 8

VANADIUM COMPONENT DEMO

8. VANADIUM COMPONENT DEMO

Vanadium alloys are considered a viable structural material for fusion power plants because of their low activation and favorable material properties. Under the Advanced Fusion Technology program, small vanadium alloy components and vanadium alloy coupons were fabricated, installed in the DIII–D tokamak and are being exposed to the thermal cycling and radiation accompanying DIII–D operations. The near-term goal is to determine structural and chemical effects on candidate vanadium alloys.

In FY99, vanadium components were designed, fabricated and installed in the DIII–D vacuum vessel. The components, small strut protection tile assembly brackets (Figs. 8-1 and 8-2), consist of two milled vanadium alloy plates that have been electron beam and gas tungsten arc welded. The vanadium welding techniques were developed by ORNL as part of an ORNL, ANL and GA collaboration. A total of six protection tile bracket assemblies were installed in DIII–D. Tensile and impact specimens were installed adjacent to the bracket assemblies to allow for the monitoring of the parent and welded material properties without having to remove the brackets for analysis/destructive testing.

Samples are to be removed after one and three years of exposure, matching the effective exposure for the ANL vanadium alloy data.

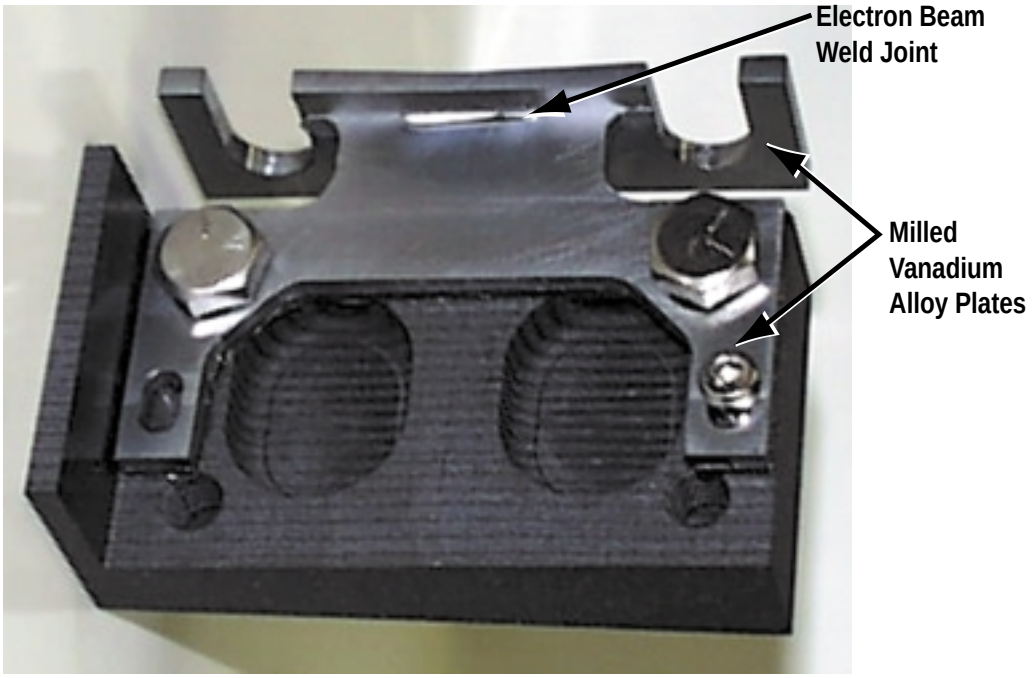

Fig. 8-1. Vanadium brackets are part of the DIII–D strut protection tile assemblies.

In FY00, after one year of exposure, one set of samples were removed. These parent and welded material samples will be analyzed by ANL during FY01. When analyzed, these specimens will provide fracture toughness, ductile-to-brittle transition temperature, yield strength and ultimate tensile strength material data. The next removal of vanadium alloy samples will be in FY02.

Initial discussions were held with the Japanese National Research Institute for Metals (NRIM) on a possible collaboration to investigate creep, fatigue and creep-fatigue behavior of vanadium alloy after exposure to a radiation environment.

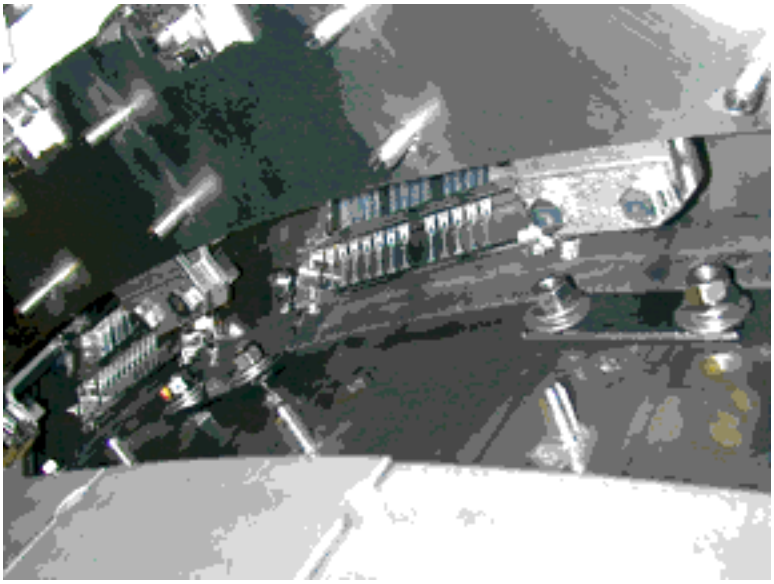

Fig. 8-2. Vanadium alloy specimens behind DIII–D private flux divertor baffle.

Section 9

RF TECHNOLOGY

Section 9

RF TECHNOLOGY

9. RF TECHNOLOGY

COMBLINE ANTENNA

During FY00, continued discussions on combline antenna design were held with staff of Japan's National Institute of Fusion Science and with Prof. Takase of the University of Tokyo. NIFS has a collaboration with Prof. Takese to assist in the design and fabrication of a combline antenna for the LHD device. NIFS is considering a combline antenna to be located in the high magnetic field region of the stellerator to achieve good coupling with the electrons for fast wave current drive.

Discussions were held at NIFS on October 5, 1999 with Prof. Takase and Dr. Watari and his staff. Their modular combline antenna design, which is well suited to following a twisted helical path on the LHD, was reviewed, and GA staff were able to help clarify some model measurements, as well as make suggestions regarding the Faraday shield design. At that time, Prof. Takase was proposing to use inductive coupling to drive one half of the antenna array. GA staff proposed a configuration for efficient coupling in such an antenna configuration and proposed to test the approach using a mockup already existing at GA.

GA analyzed and performed experiments on an existing combline antenna mockup at GA to test two schemes for coupling rf power to the antenna. One of the approaches, which had been discussed with Prof. Takase, was to use an inductive loop to couple with the combline antenna. The other approach is to use direct feed to the antenna element in a way that excites the evenly distributed current on the antenna elements. The results of the theoretical analyses and experimental results on both approaches were documented in a report titled “Combline Antenna with Half-Wavelength Elements,” which was provided to NIFS and Prof. Takase. The experiments at GA showed that the coupling efficiency using the inductive approach is quite low. The direct coupling approach tested at GA gave good impedance characteristics, enabling operation without an impedance matching section over a wide range of frequencies with and without plasma loading. The apparatus used in the experiments, including a combline antenna mockup and a water load to simulate absorption in a plasma, is shown in Fig. 9.1.

Prof. Takase made a 4-strap combline for testing the concept. The design initially used the inductive loop coupling approach, but experiments showed that the inductive coupling was weak. Prof. Takase indicated he would like to try direct coupling. GA staff plan to visit Japan in November 2000 to explore improved means of coupling rf power to the 4-strap antenna.

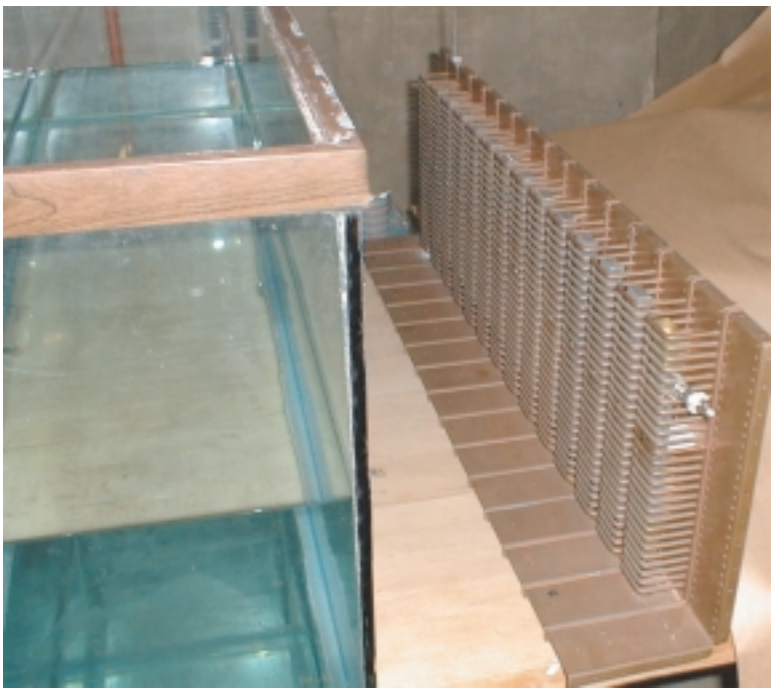

Fig. 9.1. GA combline antenna mockup and water load.

ADVANCED ECH LAUNCHER DEVELOPMENT

Improved launcher mirror concepts with enhanced heat removal capability are being developed. Three main concepts were evaluated during FY00. All three concepts use inexpensive carbon fibers as the heat sink and/or heat pipe to a heat sink. Carbon fibers offer the advantage of flexibility that enables the rotating mirror to be connected with a flexible heat pipe to a fixed cooled heat sink. The three concepts evaluated were: a) copper-coated graphite mirror, b) copper-coated molybdenum brazed to a carbon fiber composite (CFC) disk, and c) copper-coated CFC disk. Thermal analyses show that a graphite mirror with a graphite fiber cooling braid connected to a water-cooled heat sink can operate with 10 s 900 kW pulses with less than 5 min cool-down time between shots.

Thermal analyses show that copper-coated molybdenum brazed to a carbon fiber composite (CFC) substrate mirror can meet the 10 s pulse length criterion. For a 2.5 cm thick CFC substrate, 0.8 MW 10 s pulses every ten minutes result in a maximum surface temperature of 540°C, even without a carbon fiber umbilical cord attached. Such an umbilical cord would reduce the maximum surface temperature and increase the permissible repetition rate.

Thermal analyses were also performed for the design using a copper-coated CFC disk with a high thermal conductivity flexible carbon fiber bundle heat pipe emanating from

the backside. The analysis shows that a DIII–D size mirror can reflect 1 MW for about two minutes before the hottest spot exceeds 200°C, with a starting temperature and heat sink temperature of 35°C. The carbon fiber bundle diameter in this design is 6 cm and the fiber length is 20 cm. With a larger bundle of fibers to the heat sink, true CW can be achieved. The carbon fibers used in this design have an axial thermal conductivity close to that of CVD diamond, i.e. about 100 W/m-K. The CFC disk consists of unidirectional fibers of 66% to 80% volume density embedded in a graphite composite having a transverse thermal conductivity of 50 to 100 W/mK. A proof-of-principle experiment for this design was developed. An order was placed with a vendor to fabricate a CFC disk with an integral bundle of fibers emanating from the back. This mirror is designed to fit a standard DIII–D miter bend frame for testing. The fiber bundle diameter for this experiment is only 1.3 cm in order to keep costs within budget. The prototype assembly was received at the end of the fiscal year and was sent to a vendor to apply a dense CVD carbon layer on the mirror surface prior to applying a copper coating.

In a related development, GA conducted initial low power tests on its company-funded proof-of-concept remotely-steerable 110 GHz ECH launcher. The tests successfully demonstrated that steering of ± 15° can be achieved with this concept. Low power tests were also successfully carried out on this launcher with miter bends included between sections of launcher waveguide. These tests showed that the predicted steering can be achieved with or without miter bends. The "folded" waveguide has the bends out of the plane of steering.

JAERI has considerable interest in the remotely steeriable launcher concept and purchased from GA a prototype launcher suitable for high power tests at 170 GHz using evacuated launcher waveguide. The apparatus included a water-cooled rotating mirror housed in a five-way cross vacuum chamber and a 5 m long, square cross section evacuated waveguide. As part of the U.S./Japan RF Technology Exchange, GA performed low power tests on the apparatus at GA and will participate in low and high power tests in Japan next fiscal year. The apparatus set up at JAERI for low power tests is shown in Fig. 9.2.

INTERNATIONAL COLLABORATION

The U.S./Japan RF Technology Exchange Workshop was held at Oharai, Japan in October 1999 in conjunction with the EC-11 Meeting. GA staff presented papers on LHD combline antenna design, fast ferrite tuner development and testing, and remotely-steerable ECH launchers. Ongoing and potential new U.S./Japan rf collaborations were discussed. Following the workshop in Japan, the U.S. delegation, with representatives

from ORNL, PPPL, and GA, visited several sites in Korea to hold discussions on potential U.S./Korea collaborations in the area of rf heating technology. Sites visited included Kwangwoon University (Seoul), KBSI, KAIST, KSTAR (Taejon), and POSTECH (Pohang). Potential collaborative activities in ICRH and LHCD antenna design and operation were identified.

The next U.S./Japan RF Technology Exchange Workshop was planned for October 30 to November 1, 2000 at PPPL. This workshop will be held in the week immediately after the APS meeting in Quebec, Canada.

CONFERENCES/MEETINGS

1. The 18th U.S./Japan RF Technology Exchange Workshop, Oharai, Japan, October 1999.

PUBLICATIONS/REPORTS

1. H. Ikezi, "Combline Antenna with Half-Wavelength Elements," General Atomics Report GA-C23396, June 2000.

Fig. 9.2. Remotely steerable launcher apparatus in low power testing at JAERI.

Section 10

IFE TARGET SUPPLY SYSTEM

10. IFE TARGET SUPPLY SYSTEM

BACKGROUND

A commercial Inertial Fusion Energy (IFE) power plant must place about 500,000 cryogenic targets each day (at a rate of 5–7 Hz) into a target chamber operating at 500–1500°C. The targets will be injected into the reaction chamber at high speed, tracked and hit, on the fly, with the driver beams. This must be done with high precision, high reliability of delivery, and without damaging the mechanically and thermally fragile targets. Key components of demonstrating a successful IFE target injection methodology are:

- Ability of targets to survive the chamber environment (target heating due to radiation and chamber gases)
- Accuracy and repeatability of target injection and tracking (ability to provide suitable beam steering and/or target steering, and shot-timing signals)
- Ability of targets to withstand acceleration into the chamber (strength of target components, including the DT itself)

The ultimate goal of this development program is to provide a successful demonstration of injecting prototypical IFE cryogenic targets into a surrogate chamber that is representative of an operating reaction chamber.

FY00 SCOPE AND OBJECTIVES

The FY00 GA workscope for this task was focused on initiating the design of a new injection and tracking system for higher precision, multi-shot, injections of direct and indirect drive targets. We also continued analysis of numerous issues associated with target injection, tracking, and fabrication.

Brief highlights of the FY00 progress and accomplishments are covered in the following sections.

TARGET INJECTION AND TRACKING SYSTEM CONCEPTUAL DESIGN

The target injection and tracking experimental system conceptual design and Conceptual Design Review were completed. A simplified schematic drawing of the experimental system is shown in Fig. 10-1. The targets are accelerated in a gas gun. The

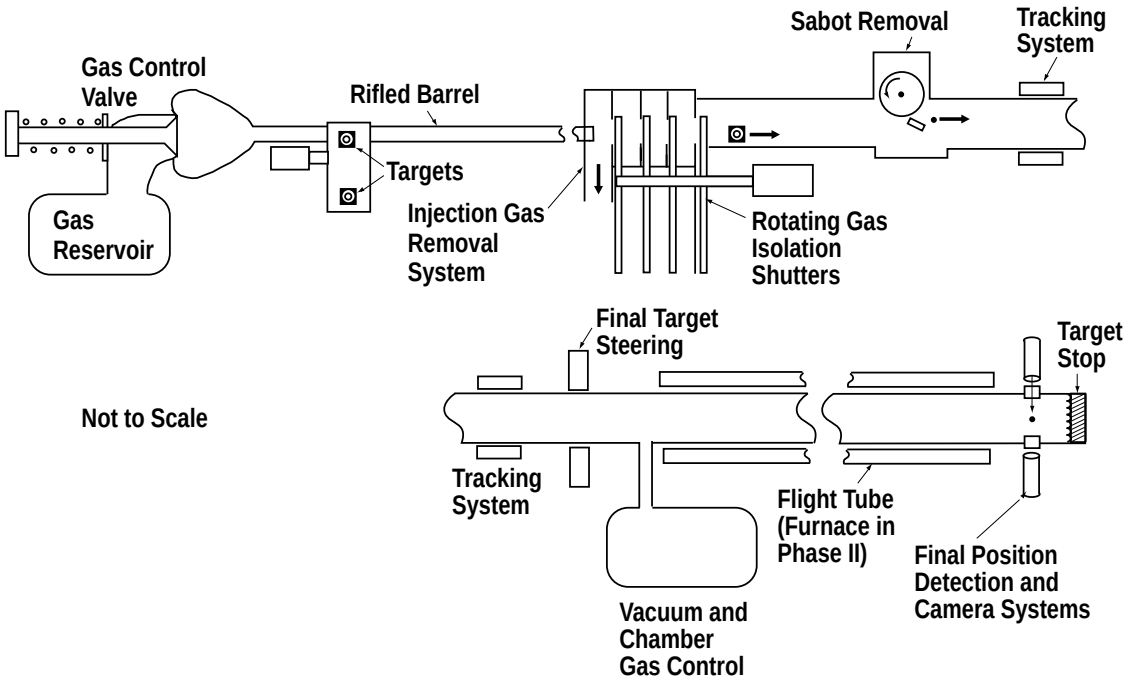

Fig. 10-1. Simplified schematic of experimental target injection and tracking system.

propellant gas and sabot are removed prior to target tracking. The targets pass two detector stations, whose output is used to predict later target trajectory. Target steering based on this position prediction may be added to improve target accuracy. There are final target position measurements to verify position prediction accuracy.

The conceptual design includes preliminary piping and instrumentation drawings, process flow diagrams, assembly drawings, instrumentation, control, and electrical diagrams. Subsystem mechanical drawings and sketches were prepared for the propellant gas control valve, the target loading station, the gas gun sabot, the injector gas removal, and the injector testing tube furnace. The tracking system design included transverse position detection using linear photodiode arrays for the first two detector stations and 2-D arrays for the final detector station. Axial position timing methods use single linear photodiode detectors, up/down counters, time to digital converters and digital delay generators to predict target arrival time to the final position prediction detectors.

The Conceptual Design Review (CDR) meeting for the target injection and tracking system was held on September 27, 2000. A five-member design review committee was selected from persons who had not worked on this project. Quoting from the Chairman's Report: “The committee concluded, based on the review of the design review package and the meeting discussions, that the design presented was a reasonable approach and was adequately developed for the conceptual design stage. The committee identified no major

issues that were not addressed by the project personnel." A number of improvements in the design were suggested by the committee and are being evaluated by project personnel.

SABOT SEPARATION EXPERIMENT

An outer structure called a sabot is required to thermally and mechanically protect a direct drive IFE target during acceleration in a target injector. The sabot must be removed from the target after it leaves the injector and then must be directed away from the driver beams. This sabot design has an internal spring that will be compressed by sabot inertia during target acceleration, then cause the sabot parts to separate axially after acceleration in the injector. A side view of the proposed direct drive target sabot design is illustrated in Fig. 10-2.

We performed a preliminary test of the sabot separation. Since the tests were conducted in air (instead of vacuum), small holes were drilled in the sabot to allow unrestricted air flow. A plastic ball was placed inside the sabot. The sabot was compressed between the arms of two high-speed springs. Upon release of the springs, the sabot separation was captured with a high-speed video camera. One frame taken 5 ms after the sabot release is shown in Fig. 10-3. The plastic ball inside the sabot is nearly motionless. A video of the separation is available on the internet at http://aries.ucsd.edu/ARIES/WDOCS/IFE/sabot.html.

This is the first in a series of sabot separation experiments. Additional and more challenging tests will involve separation of high-speed sabots from lower mass targets in a vacuum environment, and finally separation at cryogenic temperatures.

CALCULATIONS OF TARGET HEATING AND DRAG

We have implemented a computational fluid dynamics code [1,2] which utilizes the Direct Simulation Monte Carlo (DSMC) method to model the interaction of the target

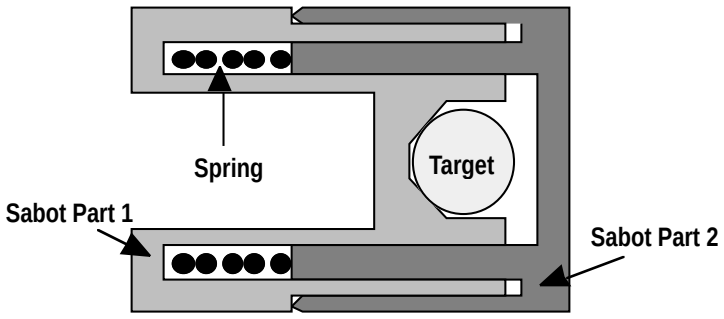

Fig. 10-2. The sabot isolates the capsule from warm propellant gas during acceleration and separates due to spring force after leaving the barrel.

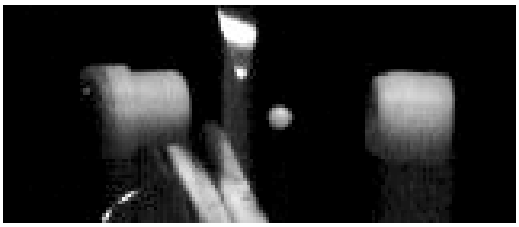

Fig. 10-3. Photograph taken 5 ms after sabot release.

with the chamber fill gas during injection. The program provides the magnitude and distribution of heating around the surface of the target. It also calculates the pressure on the target surface and the drag that acts on the target.

We calculated convective heat flux for chamber temperature of 900 K, 1373 K, and 1758 K, for target speeds of 200 m/s to 1000 m/s, and xenon densities that correspond to 0.5 mTorr to 0.5 Torr at standard temperature. We then calculated total heat flux (convection plus radiation) and the temperature rise that would occur at the surface of a NRL radiation preheat direct drive target that passes through a 6.5 m radius chamber. The heating is excessive for higher gas densities. The heating is only acceptable for the lower temperature chambers, high target reflectivity, and very low gas densities. Figure 10-4 shows the calculated target temperature change based on 98% target reflectivity and an initial temperature of 18 K. The triple point of DT is 19.7 K and temperature increases greater than 0.8 K may overstress the fuel and cause unacceptable surface roughening.

The drag force on 2 mm radius target traveling through xenon gas was also calculated. Then using the drag force, the distance the sphere traveled was calculated using the equations of motion. With the target traveling at a speed of 400 m/s, the drag

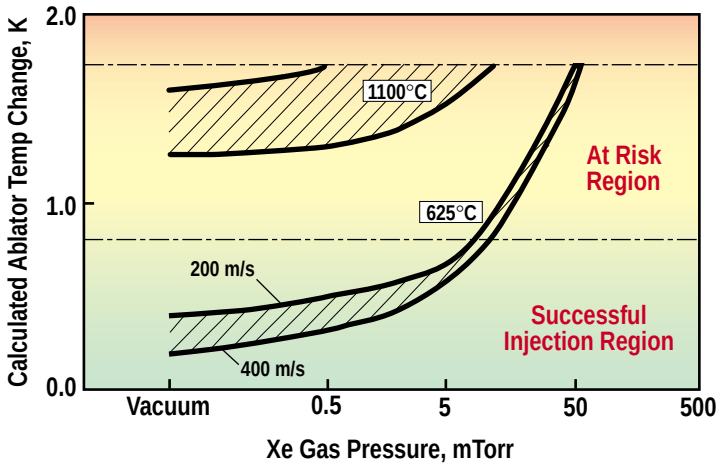

Fig. 10-4. Average target increase of outer ablator temperature for a target moving through a xenon-filled reaction chamber.

force on the sphere is approx. 0.0057 N. The calculated drag forces have a large effect on final target position. Figure 10-5 shows the effect of variations of chamber gas density on the position of the target as it approaches the chamber center. It assumes a 4 mg, 4 mm diameter target passing through a 6.5 m radius chamber at 400 m/s. A 1% density variation from 0.5 Torr causes a 1400 μm change in target position. Even 5 mTorr gas density would have to be consistent to about ± 0.1%. In-chamber target tracking could potentially measure the effect of chamber gas on target trajectory, allowing beam steering to compensate for the perturbed target position.

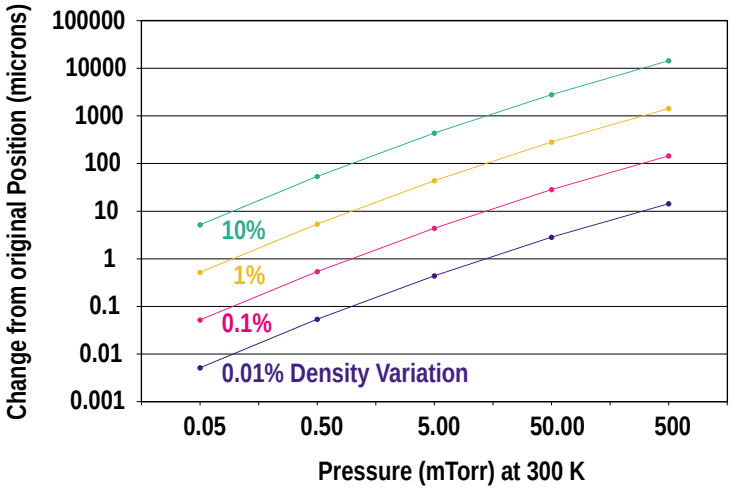

Fig. 10-5. Change in target position versus pressure for various fractional pressure variations.

SUMMARY OF ACCOMPLISHMENTS

Specific FY00 accomplishments are listed below.

1. Wrote the system design description and the design requirements basis documents with broad input from the IFE community;
2. Performed analytical reflectivity estimates for IFE targets with an optically thick gold layer averaged over all angles of incidence and a black body chamber spectrum;
3. Performed thermal analysis of IFE targets leading to a Master's Degree Thesis [3];
4. Carried out gas flow calculations for the gas from a gas gun through a series of shutters and baffle chambers. These calculations support the experimental design which requires a gas density change downstream of the first target detector of less than 4×10^{-8} kg/m^3 during a 12 shot burst;

5. Conducted preliminary calculations for indirect drive target stress induced by acceleration. These calculations assumed a thin walled cylindrical geometry;
6. Completed the target injection and tracking experimental system conceptual design and conceptual design review. This design includes many accomplishments including those discussed earlier under the conceptual design heading;
7. Conducted direct simulation Monte Carlo modeling of the thermal and drag interactions between the target and the gas in the target chamber over a range of gas pressures and temperatures;
8. Updated the target sabot design and designed a sabot latching mechanism. Calculated the expected and allowed gas leakage into the sabot, then experimentally tested the leakage into a prototype sabot. Conducted preliminary sabot separation testing;
9. Prepared thin film samples simulating the surface of a direct drive radiation preheat target. Measured the optical properties for use in calculating target reflectivity.

REFERENCES

[1] G.A. Bird, Molecular Gas Dynamics and the Direct Simulation of Gas Flows, Oxford University Press, 1994.

[2] G.A. Bird, "General Program for the Computation of Two-Dimensional or Axially-Symmetric Flows by the Direct Simulation Monte Carlo (DSMC) Method, The DS2G Program Users Guide," Version 3.2, G. A. B. Consulting, 5 Fiddens Wharf Road, Killarra, N.S.W. 2071, Australia, http://www.gab.com.au/, June 1999.

[3] N.P. Siegel, "Thermal Analysis of Inertial Fusion Energy Targets," Masters Thesis, San Diego State University, May, 2000.

CONFERENCES/MEETINGS

1. Thirteenth Target Fabrication Meeting, Catalina, California, November, 1999. Papers were presented on "Status of Target Injection and Tracking Studies for Inertial Fusion Energy," and "IFE Program – Technology Development Activities and Plans."
2. Second Japan-U.S. Workshop on Inertial Fusion Energy, Osaka, Japan, November 1999. Paper were presented on "IFE Target Injection and Tracking" and "Mass Production of Inertial Fusion Energy Targets."

3. Thirteenth International Symposium on Heavy Ion Inertial Fusion, San Diego, California, March, 2000. A paper was presented on "IFE Target Fabrication and Injection – Achieving "Believability."
4. IAEA Technical Committee Meeting on Physics and Technology of Inertial Fusion Energy, Madrid, Spain, June, 2000. A paper was presented on "Developing the Basis for Target Injection and Tracking in Inertial Fusion Energy Power Plants."

PUBLICATIONS/REPORTS

1. R.W. Petzoldt, D.T. Goodin, and N.P. Siegel, "Status of Target Injection and Tracking Studies for Inertial Fusion Energy," Fusion Technology, Vol. **38**, No. 1, (2000) pp. 22–27.
2. R.W. Petzoldt, "Target Injection and Tracking System Design Requirements Basis," GA-0001-02DR, May, 2000.
3. R.W. Petzoldt, "Target Injection and Tracking Design Description," GA-7-0001-01DD, May, 2000.
4. N.P. Siegel, "Thermal Analysis of Inertial Fusion Energy Targets," Masters Thesis, San Diego State University, May, 2000.
5. M. Dunlap, "Quality Assurance Program Document – Inertial Fusion Energy Target Injection and Tracking Program," GA-QAPD-30007, September, 2000.
6. W. Egli, "Technical Specification for Fast Acting Gas Valve," GA-7-0001-03TS-A, September, 2000.

Section 11

ARIES INTEGRATED SYSTEM STUDIES

11. ARIES INTEGRATED SYSTEM STUDIES

BACKGROUND

The ARIES Program is a multi-institutional activity to explore and develop the commercial potential of fusion as a future energy source. This is accomplished through integrated systems studies of both MFE and IFE power plant concepts. General Atomics' task is to provide target injection and target fabrication input to the ARIES-IFE integrated system studies.

ACCOMPLISHMENTS AND ACTIVITIES

GA participated in the ARIES-IFE study kickoff meeting in Madison on June 19–21, 2000. Heating of targets during injection through the chamber fill gas was identified as a major issue.

Two viewgraph packages were prepared and presented at the meeting. The first one, "Target Selection for ARIES-IFE" recommended evaluating four classes of targets in the system study: the direct-drive shock preheated design, the direct-drive radiation preheated target, the indirect-drive x-ray driven target and the indirect-drive close-coupled, distributed radiator design. The second presentation, "Developing the Basis for Target Injection and Tracking in Inertial Fusion Energy Power Plants," concluded that target heating for the close-coupled indirect-drive target was negligible but that the radiation preheated direct-drive target would be significantly degraded by thermal exposure during injection.

GA participated in the ARIES-IFE study meeting in Princeton on September 18–20, 2000.

Three viewgraph packages were prepared and presented at the meeting. The first one, "IFE Target Fabrication Plans and Progress" discussed both indirect drive and direct drive target fabrication. An overview of the fabrication development plans was presented, which involves both the development of new methods and the adaptation of existing ICF technologies for IFE. The objective is to show a credible pathway for IFE target fabrication.

The second presentation, "Target Injection in a Gas-Filled Chamber," reiterated that the reference gas pressure in the SOMBRERO chamber resulted in excessive heating of the target and target drag during injection, then presented parametric calculations of acceptable gas pressures and temperatures for target survival. Given the current target

design, and without additional protection, a reduction in gas pressure of about two orders of magnitude (to ~5 mTorr) and a reduction in first wall temperature to about 625°C would be needed to ensure target survival.[1] Evaluations of increasing the polymer shell thickness of the direct drive target showed that about 200 μm would be needed to provide significant insulation capability in this environment. Such a thickness is inconsistent with the current target physics design.

The third presentation, "Design of the Target Injection and Tracking Experimental System" discussed the technology development strategy, the injection and tracking requirements, and the conceptual design of the system.

CONFERENCES/MEETINGS

1. ARIES-IFE Study Kickoff Meeting, Madison, Wisconsin, June 19–21, 2000.
2. ARIES-IFE Study Meeting, Princeton, New Jersey, September 18–20, 2000.

[1] A concept to reduce the first wall temperature while maintaining the energy conversion efficiency was brought up and discussed at this meeting. Since a significant amount of the fusion energy is released as neutrons which are not absorbed by the first wall, "overcooling" of the first wall (e.g., to 625°C) may be possible.

Section 12

SPIN-OFF BROCHURE

12. SPIN-OFF BROCHURE

Over the last fifty years the pursuit of fusion energy has led to the development of materials, processes, codes and understanding of basic plasma physics that have found many applications in scientific and engineering fields outside of the fusion arena. GA has written a brochure illustrating ways that fusion science and technology have influenced and contributed to these other fields. The brochure is sixteen pages long and targets the interested but non-technical person, with an effort to provide a basic understanding of the fusion process and the contribution fusion research has had on other technologies and scientific areas. In addition to the normal "spin-off" topics usually applied to such literature, the concept of highly trained experts as a spin-off commodity has been included. The migration to other research fields by fusion experts, with their broad understanding of the very complex phenomena occurring in the study of heated plasmas, may be the largest impact fusion research has had on other scientific fields.

The title of the brochure is "The Unpredictable Benefits of Creating a Star". After the introduction the brochure gives a brief description of the three known methods of achieving conditions for sustained fusion to occur. The section on inertial fusion is shown in Fig. 12-1.

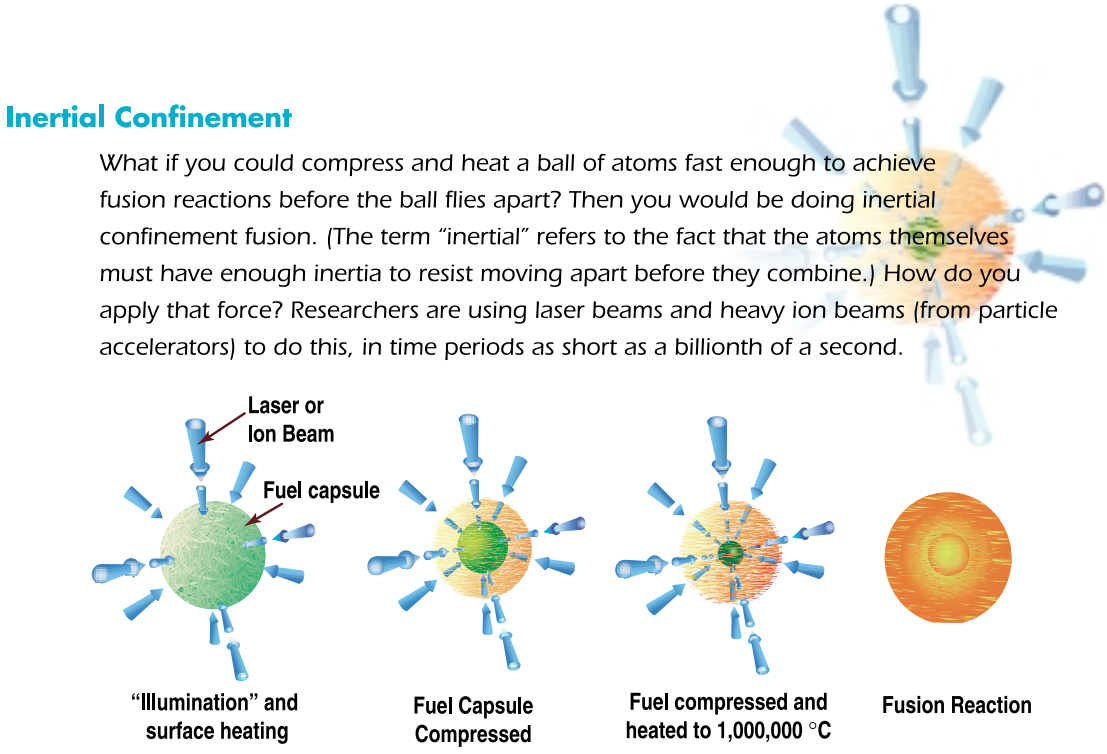

Fig. 12-1. The spin-off brochure begins with explanations of fusion aimed at the interested but non-technical person.

The next part of the brochure covers the areas of physical science that have seen contributions from the fusion program. High density material science and nonlinear chaotic system behavior are identified as areas with much synergism. The remainder of the brochure covers technology spin-offs, such as space travel, semiconductor circuit fabrication, material processing, medical and health applications, and pollution reduction and remediation.